Komatsu and Yokoyama *J Wood Sci* (2021) 67:45
https://doi.org/10.1186/s10086-021-01978-4

Journal of Wood Science

ORIGINAL ARTICLE

Open Access

Revisiting the condensation reaction of lignin in alkaline pulping with quantitativity part I: the simplest condensation between vanillyl alcohol and creosol under soda cooking conditions

Toshihiro Komatsu and Tomoya Yokoyama*

Abstract

The condensation reaction of lignin is believed to interfere with delignification in alkaline pulping processes, without any clear evidence, which has motivated us to quantitatively revisit it. This paper is the first of a series, and hence we employed the simplest model system using 4-hydroxymethyl-2-methoxyphenol (vanillyl alcohol, Va) and 2-methoxy-4-methylphenol (creosol, Cr) under soda cooking conditions. The *α*-5-type condensation product between these compounds [VaCr, 2-(4-hydroxy-3-methoxybenzyl)-6-methoxy-4-methylphenol] was identified and quantified as exclusive. VaCr was yielded with a mole amount of 24%, 46%, 62%, or 72% based on that of disappearing Va at a reaction time of 120 min when the ratio of the initial concentration of Cr to that of Va was 1.0, 2.5, 5.0, or 7.5, respectively. These yields and an HPLC analysis of the reaction solution obtained by a treatment of Va as the sole compound under the same soda cooking conditions suggested the formation of self-condensation products of Va even in the treatments containing Cr. The obtained results comprehensively suggested that the self-condensation of Va progresses more readily than the condensation between Va and Cr. The factors behind this will be the topic of our next paper.

Keywords: Alkaline pulping, Condensed structure, Delignification, Quinone methide

Introduction

Condensation is a major reaction mode of phenolic substructures of lignin in alkaline pulping processes. Figure 1 illustrates these condensation reactions of lignin on the basis of previous reports by Gierer et al. [1–4], although they often employed compounds that are not appropriate as lignin models. First of all, condensation progresses only between phenolic substructures. The primary reaction is the liberation of the hydroxide anion (HO^-) from the benzyl position (*α*-position) of a dissociated phenolic (phenoxide) substructure to afford the important intermediate, a quinone methide structure (QM, Fig. 1). The aromatic nucleus of another phenoxide substructure nucleophilically attacks the *α*-carbon of QM to afford an *α*-5- or *α*-1-type condensation product. The side-chain portion is released as an aldehyde fragment in the formation of the latter type. Formaldehyde (HCHO) is often liberated from a *γ*-hydroxymethyl group during the processes, and reacts with the aromatic nucleus of a phenoxide substructure to introduce a hydroxymethyl group on the empty *ortho*-position. This *ortho*-hydroxymethylated substructure similarly liberates the HO^- to convert to the *ortho*-type QM (*o*-QM, Fig. 1), which is also nucleophilically attacked by the aromatic nucleus of another phenoxide substructure to afford a 5-CH_2-5-type product.

*Correspondence: yokoyama@woodchem.fp.a.u-tokyo.ac.jp
Laboratory of Wood Chemistry, Department of Biomaterial Sciences, Graduate School of Agricultural and Life Sciences, The University of Tokyo, 1-1-1 Yayoi, Bunkyo-ku, Tokyo 113-8657, Japan

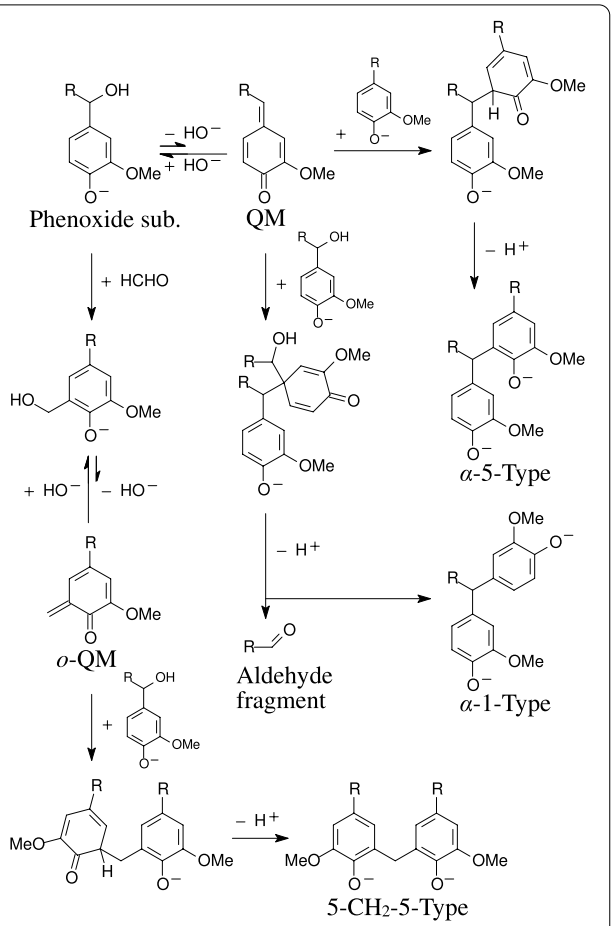

Fig. 1 Condensation reactions of lignin shown in previous reports [1–4]

The *α*-5-type condensation reaction was confirmed to actually progress in an alkaline treatment of two guaiacyl-type compounds, 4-hydroxymethyl-2-methoxyphenol (vanillyl alcohol) and 2-methoxy-4-methylphenol (creosol), by detecting 2-(4-hydroxy-3-methoxybenzyl)-6-methoxy-4-methylphenol, the *α*-5-type condensation product between these compounds [5]. The *α*-1-type condensation was confirmed to actually progress in an alkaline treatment of a *p*-hydroxyphenyl type compound, 4-hydroxymethylphenol, by detecting bis(4-hydroxyphenyl)methane, the *α*-1-type condensation product between two molecules of this compound, accompanying the release of the HCHO molecule [6]. This *α*-1-type condensation product was detected with an amount of about 70–80% of the *α*-5-type condensation product, 2-(4-hydroxybenzyl)-4-hydroxymethylphenol [6]. A guaiacyl-type compound, vanillyl alcohol, afforded the *α*-1-type condensation product, bis(4-hydroxy-3-methoxyphenyl)methane, together with trimers and molecules larger than trimers generated by the *α*-1- and *α*-5-type condensation reactions of vanillyl alcohol in an alkaline treatment [7, 8]. A syringyl type compound, 4-hydroxymethyl-2,6-dimethoxyphenol (syringyl alcohol), also afforded the *α*-1-type condensation product, bis(4-hydroxy-3,5-dimethoxyphenyl)methane, in an alkaline treatment [9]. The 5-CH_2-5-type condensation was confirmed to actually progress in an alkaline treatment of creosol and HCHO [5, 10] or of 2-hydroxymethyl-6-methoxy-4-methylphenol (5-hydroxymethylcresol) alone [11] by detecting bis(2-hydroxy-3-methoxy-5-methylphenyl)methane, which was produced by the 5-CH_2-5-type condensation between two molecules of creosol and HCHO or between two molecules of 5-hydroxymethylcreosol releasing the HCHO molecule, respectively.

The condensation products were confirmed to be stable under alkaline conditions, using the *α*-5-type product between vanillyl alcohol and creosol, 2-(4-hydroxy-3-methoxybenzyl)-6-methoxy-4-methylphenol, the *α*-1-type product between two molecules of vanillyl alcohol, bis(4-hydroxy-3-methoxyphenyl) methane, and the 5-CH_2-5-type product between two molecules of creosol and HCHO, bis(2-hydroxy-3-methoxy-5-methylphenyl)methane [12, 13].

It was thus confirmed that the *α*-5-, *α*-1-, and 5-CH_2-5-type condensations actually progress and that the condensation products are stable under alkaline conditions. As the progress of condensation is accompanied by polymerization of lignin, it has been considered to be undesirable for delignification in alkaline pulping processes. This undesirability is further reinforced by the fact that residual lignin in pulp or lignin-originating organic compounds in black liquor, whose structures are not well understood, affords only small amounts of vanillin and its analogues in the alkaline nitrobenzene oxidation method, although low yields of these compounds do not show abundance of condensed substructures in the lignin samples but only absence of the uncondensed substructure.

However, there are several issues with unquestioningly concluding that condensation is absolutely undesirable for delignification. The above-described knowledge is not quantitative but qualitative. Gierer and Ljunggren showed that a trimeric lignin model compound of *α*-5-type condensation product carrying the *β*-*O*-4 bond undergoes the *β*-*O*-4 bond cleavage much more readily than a common dimeric *β*-*O*-4-type lignin model compound, owing to the ready neighboring group participation of the phenoxide of the condensed aromatic nucleus (Fig. 2) [14]. Although this finding originates from model experiments and hence cannot be directly applied to an actual alkaline pulping process, it suggests that the *β*-*O*-4 bond is more readily cleaved when a common phenolic *β*-*O*-4-type substructure condenses at its aromatic C-5

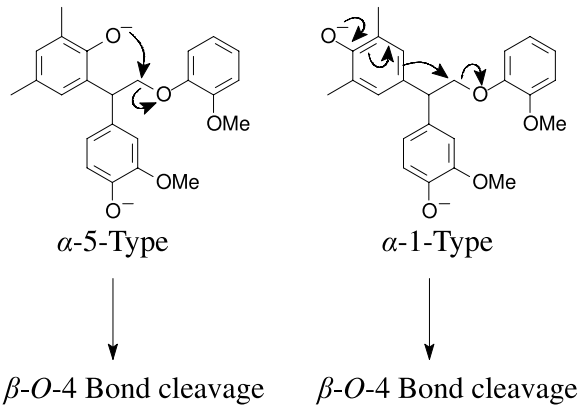

Fig. 2 Progress of the *β-O*-4 bond cleavage in model compounds of the *α*-5- and *α*-1-type condensation substructures [14]

position to convert to an *α*-5-type condensed substructure with the *β-O*-4 bond. In other reports, *α*-5-type condensation substructures are primarily generated by an acidic pretreatment together with *p*-cresol to enhance the neighboring *β-O*-4 bond cleavage in a following alkaline cooking process [15–20]. It was also shown that an analogous trimeric model compound of *α*-1-type condensation product undergoes *β-O*-4 bond cleavage, although the rate is lower than that of a common dimeric *β-O*-4-type lignin model compound. Therefore, the *α*-1-type condensation does not strongly interfere with the cleavage of the neighboring *β-O*-4 bond (Fig. 2) [14]. It is thus unclear whether the progress of condensation reactions invariably interferes with delignification in alkaline pulping processes, and we were motivated us to quantitatively revisit the condensation reactions in these processes.

Because this paper is the first in a series, the simplest system was employed. Two guaiacyl-type phenolic lignin model compounds, vanillyl alcohol (**Va**, Fig. 3) and creosol (**Cr**, Fig. 3), were treated together under soda cooking conditions. The disappearances of **Va** and **Cr** were examined in detail, with identification and quantification of the condensation products.

Materials and methods

Materials

All chemicals were purchased from Fujifilm Wako Pure Chemical Industries Co. (Osaka, Japan), Tokyo Chemical Industry Co., Ltd. (Tokyo, Japan), or Sigma-Aldrich Japan K. K. (Tokyo, Japan), and used without further purification except for **Va**. **Va** was recrystallized from methanol (MeOH) before use. High purity of **Va** and **Cr** were confirmed by ^{1}H-NMR (JNM-A500, 500 MHz, JEOL Ltd., Tokyo, Japan) before use. Deionized water (H_2O) was used.

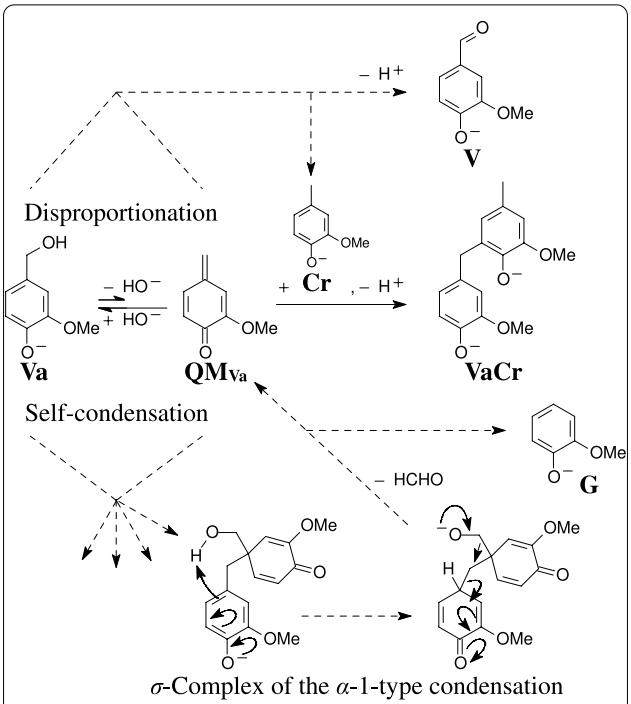

Fig. 3 Possible reactions suggested to progress in this work. Dotted lines show reactions whose occurrences have not completely been confirmed

Soda cooking for isolation and identification of condensation product

A solution (100 mL) was prepared containing sodium hydroxide (NaOH, 1.06 mol/L), **Va** (10 mmol/L), and **Cr** (50 mmol/L), to simulate a soda cooking process. A portion of the solution (5.0 mL) was transferred into a stainless-steel autoclave (10 mL volume, Taiatsu Techno® Co., Tokyo, Japan), and the air present in the head space was replaced with nitrogen gas. A further 19 autoclaves with exactly the same contents were simultaneously prepared. All 20 autoclaves were immersed together in an oil bath at 150 °C and left soaking with shaking.

After 240 min, all the autoclaves were taken out, immediately immersed in an ice/water-bath, and then the content of each was neutralized with acetic acid (AcOH, 0.6 mL). The combined neutralized solution was extracted with dichloromethane three times and then once with ethyl acetate (EtOAc). The combined organic layer was washed with H_2O and brine, dried over anhydrous sodium sulfate, and concentrated by an evaporator under reduced pressure to afford a brown syrup (776 mg). The syrup was fractionated by preparative thin layer chromatography (PTLC) using *n*-hexane/EtOAc mixture (2/1) as the eluent. A crystal (102 mg) was obtained from an area of the PTLC surface, where a condensation product could exist, by extraction of the

area with EtOAc and successive evaporation. The crystal was recrystallized from 50% aqueous MeOH, which afforded a white needle crystal (87 mg).

The obtained needle crystal was dissolved in acetone-d_6 with an aliquot of deuterium oxide, and then analyzed by ^{1}H-NMR, ^{13}C-NMR (JNM-A500, JEOL Ltd.), ^{13}C-NMR DEPT135, 2D-NMR ^{1}H-^{1}H COSY, 2D-NMR ^{1}H-^{13}C HSQC, 2D-NMR ^{1}H-^{13}C HMBC, and LC/MS (LC-2010C$_{HT}$/LCMS-2020, Shimadzu Co., Kyoto, Japan). Conditions for the HPLC portion of the LC-2010C$_{HT}$ apparatus were as follows: an HPLC column, Luna 5 µm C18(2) 100 Å (length: 150 mm, inner diameter: 4.6 mm, particle size: 5.0 µm, Phenomenex, Inc., Torrance, CA, USA), was used at an oven temperature of 40 °C with a solvent flow rate of 0.2 mL/min. The solvent and gradient were MeOH/H_2O (v/v) from 15/85 to 55/45 for 10 min, from 55/45 to 75/25 for 30 min, and maintained for 10 min, giving a total time of 50 min. Electrospray ionization (ESI) was used in the MS analysis.

Soda cooking for quantitative analysis

A reaction solution (5.0 mL) was prepared containing NaOH, **Va** (10 mmol/L), and **Cr** using degassed H_2O, and transferred into the stainless-steel autoclave. Table 1 lists the initial concentrations of the contents and systems employed in this work. The air present in the head space was replaced with nitrogen gas. A further six autoclaves with exactly the same content were simultaneously prepared. All 7 autoclaves were immersed together in an oil bath with shaking at 130 °C, 150 °C, or 170 °C and left soaking for 0, 10, 20, 30, 45, 60, or 120 min with shaking. All reactions were conducted three times to confirm reproducibility.

Table 1 Reaction systems employed in this work

System	Temp (°C)	Initial concentration		
		Va[a]	Cr[a]	NaOH[b]
Cr0	150	10	0	1.010
Cr10	150	10	10	1.020
Cr25	150	10	25	1.035
Cr50	150	10	50	1.060
Cr75	150	10	75	1.085
130	130	10	50	1.060
150[c]	150	10	50	1.060
170	170	10	50	1.060

[a] mmol/L

[b] mol/L

[c] Identical system to Cr50

Quantification

One autoclave was taken out from the oil bath at each specified reaction time and immediately immersed in an ice water bath. AcOH (0.6 mL) was added for neutralization followed by addition of a MeOH solution (5.0 mL) containing the internal standard compound (IS), 4-hydroxybenzaldehyde. After thoroughly shaking the autoclave, a portion of the content was filtered with a membrane filter, and the filtrate was analyzed by HPLC (LC-2010C$_{HT}$, Shimadzu Co.) equipped with an UV–Vis detector for quantification (280 nm). Conditions for the HPLC analysis were the same as described above.

Results and discussion

Building the reaction system

The simplest system was desirable, because this is the first paper of the series. As shown in Fig. 1, QM primarily forms accompanying the liberation of HO^- from the α-position of a phenoxide substructure in an alkaline pulping process. **Va** is the simplest lignin model compound that can convert to a QM, because it has the phenolic hydroxy group, the shortest side-chain with the α-hydroxy group, and the guaiacyl nucleus that is a characteristic aromatic nucleus of lignin. QM is nucleophilically attacked by the aromatic nucleus of another phenoxide substructure to mainly afford an α-5- or α-1-type condensed substructure. An aldehyde fragment is released in the formation of the latter type. A prerequisite for the simplest lignin model compound as this nucleophile is to have a guaiacyl nucleus and a methyl group as the side-chain that does not have any hydroxy group to quench the α-1-type condensation with the QM derived from **Va** (**QM$_{Va}$**, Fig. 3). High stability under alkaline conditions is another prerequisite. **Cr** is thus the simplest lignin model compound as this type of nucleophile.

Soda cooking conditions were employed, since this is the simplest alkaline pulping process. Because the condensation between two molecules of **Va** (**Va** and **QM$_{Va}$**, self-condensation) should be suppressed as much as possible to simplify the reaction, the initial concentration of **Cr** should be higher than that of **Va**. The initial concentrations of **Va** and **Cr** were thus set to 10 and 50 mmol/L, respectively, in the isolation and identification of condensation products. In a reaction using these compounds with these initial concentrations, 60 mmol/L of NaOH is always consumed by these compounds before the soda cooking reaction progresses. Thus, the concentration of NaOH was set to be the same as the total of the initial concentrations of **Va** and **Cr** plus 1.0 mol/L in all reactions, to maintain a concentration of 1.0 mol/L after the consumption of NaOH by the initially added **Va** and **Cr**. Table 1 lists the reaction systems employed not for the

isolation and identification but for the quantitative analysis. Several different initial concentrations of **Cr** and temperatures were employed. The initial concentration of **Va** was always 10 mmol/L.

Thus, the *α*-5-type condensation product between **Va** and **Cr**, 2-(4-hydroxy-3-methoxybenzyl)-6-methoxy-4-methylphenol (**VaCr**, Fig. 3), was expected to form as the exclusive major product, at least in systems Cr50 and Cr75.

Identification of condensation product

Va and **Cr** were treated together to isolate and identify condensation products under the same conditions as system Cr50 for the quantitative analysis, except that the scale was larger than that of this system. The white needle crystal of the isolated condensation product was obtained in yields of 38 and 32 mol% before and after recrystallization, respectively, based on the initial mole amount of **Va**. In accordance with our expectation, this isolated compound was identified as **VaCr**, the *α*-5-type condensation product between **Va** and **Cr**, on the basis of all the observed NMR and MS spectra. Figure 4a, b, c, d shows the ^{1}H-NMR spectrum, its aromatic region, ^{13}C-NMR spectrum, and MS spectrum of **VaCr**, respectively. The ^{13}C-NMR DEPT135 (Additional file 1: Fig. S1), 2D-NMR ^{1}H-^{1}H COSY (Additional file 1: Fig. S2), 2D-NMR ^{1}H-^{13}C HSQC (Additional file 1: Figs. S3–S6), and 2D-NMR ^{1}H-^{13}C HMBC spectra (Additional file 1: Figs. S7–S11) are shown in the Additional file. The peaks appearing in the ^{1}H-NMR, ^{13}C-NMR, and MS spectra were assigned as below. In the following assignments, the letter 'Va-' or 'Cr-' indicates from which compound, **Va** or **Cr**, the targeted sites originated.

^{1}H-NMR: δ 2.15 (s, 3H, Cr-C$_{\alpha}$H$_3$), 3.75 (s, 3H, Va-OCH$_3$), 3.78 (s, 3H, Cr-OCH$_3$), 3.80 (s, 2H, Va-C$_{\alpha}$H$_2$), 6.47 (m(dt), 1H, Cr-aromatic C$_6$-H), 6.60 (d, 1H, J=1.9, Cr-aromatic C$_2$-H), 6.66 (dd, 1H, J=1.9 and 8.0, Va-aromatic C$_6$-H), 6.68 (d, 1H, J=8.0, Va-aromatic C$_5$-H), 6.87 (d, 1H, J=1.9, Va-aromatic C$_2$-H). ^{13}C-NMR: δ 21.0 (Cr-C$_{\alpha}$), 35.6 (Va-C$_{\alpha}$), 56.1 (Va- or Cr-OCH$_3$), 56.2 (Va- or Cr-OCH$_3$), 110.8 (Cr-aromatic C$_2$), 113.4 (Va-aromatic C$_2$), 115.4 (Va-aromatic C$_5$), 122.1 (Va-aromatic C$_6$), 123.4 (Cr-aromatic C$_6$), 128.4 (Cr-aromatic C$_5$), 128.7 (Cr-aromatic C$_1$), 133.7 (Va-aromatic C$_1$), 142.5 (Cr-aromatic C$_4$), 145.5 (Va-aromatic C$_4$), 147.8 (Cr-aromatic C$_3$), 148.0 (Va-aromatic C$_3$). MS in positive mode (detected ion, m/z (rel. int.)): 571 ([2M+Na]$^+$, 40), 329 ([M+MeOH+Na]$^+$, 24), 315 ([M+K]$^+$, 95), 297 ([M+Na]$^+$, 100). MS in negative mode (m/z (rel. int.)): 273 ([M−H]$^-$, 100).

Figure 5d shows the HPLC chromatogram of the reaction solution in system Cr50 that was performed not for isolation and identification of **VaCr** but for the quantitative analysis. All the conditions employed in system Cr50 were the same as those in the reaction for isolation and identification of **VaCr** except that the reaction was terminated at a reaction time of not 240 but 120 min and IS was added. Therefore, Fig. 5d can be substituted for the chromatogram drawn in the analysis of the reaction for isolation and identification of **VaCr**. The peak appearing at a retention time of 23.6 min corresponds to **VaCr**. Dimers and molecules larger than dimers appeared after a retention time of about 20 min. **VaCr** was thus the exclusive major condensation product, which is reasonable given that the absorptivities of the condensation products at 280 nm are not largely different from one another. **VaCr** was quantified by preparing a calibration line using this isolated and identified **VaCr** together with IS in the following contents.

Overview of the condensation in systems Cr0–Cr75

Va and **Cr** were treated under the soda cooking conditions in systems Cr0–75, where the initial concentrations of **Cr** were different, to examine how the condensation reaction differed in these systems. Figure 5a, b, c, d, e shows the HPLC chromatograms of the reaction solutions obtained at a reaction time of 120 min in systems Cr0, Cr10, Cr25, Cr50, and Cr75, respectively, after adding IS and filtration. The vertical scales were standardized by the peak heights of IS. Many peaks in Fig. 5b–e appear at the same retention times as those in Fig. 5a. Thus, self-condensation products of **Va** and disproportionation products described below must have formed even in system Cr75, where the initial mole amount of **Cr** was 7.5 times that of **Va**, although the formation of these products requires further confirmation by other methods. The peaks of **Va** are smaller with increasing initial concentration of **Cr**, indicating that **Va** condensed more rapidly with the increase. The peaks of **VaCr** are larger with increasing initial concentration of **Cr**, which indicates that **VaCr** became the more exclusive condensation product with the increase.

The peaks at retention times of 12.2 min and 13.7 min showed vanillin (**V**, 4-hydroxy-3-methoxybenzaldehyde) and guaiacol (**G**, 2-methoxyphenol), respectively. **V** was isolated from the reaction solution and identified by the retention time and structural analyses by ^{1}H-NMR and LC/MS (see Additional file 1). The authentic compound of **G** appeared at the same retention time and showed the same UV–Vis spectrum as the peak at 13.7 min when the reaction solution and authentic compound were analyzed by a photodiode array (PDA) detector (SPD-M10A, Shimadzu Co.) in the HPLC apparatus, although complete identification should be additionally conducted by other methods. **V** is presumed to have formed via a reaction route whereby **Va** is oxidized by $\mathbf{QM_{Va}}$, namely,

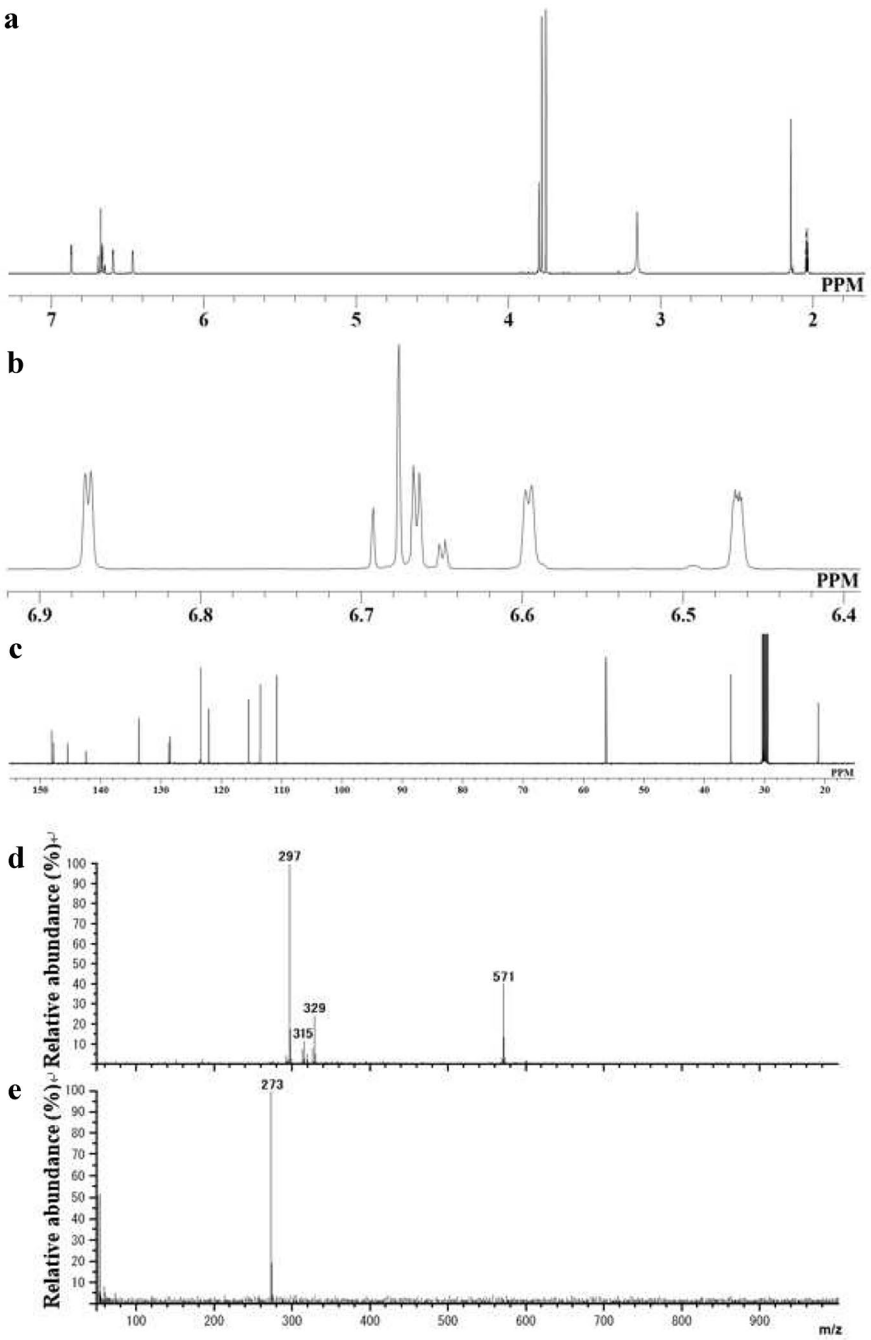

Fig. 4 Spectra of **a** ^{1}H-NMR, **b** low field region of ^{1}H-NMR, **c** ^{13}C-NMR, **d** positive mode of MS obtained by the ESI method, and **e** negative mode of MS obtained by the ESI method

the disproportionation of **Va** (Fig. 3). Several previous reports indicate that phenolic compounds can be oxidized by QMs [21–26]. The yields of **V** with standard deviations from three duplicate runs (shown in parentheses) were 4.5% (±0.4), 3.0% (±0.4), 2.5% (±0.1), 1.2% (±0.1), and 1.3% (±0.4), based on the initial mole amount of **Va** at a reaction time of 120 min in systems Cr0, Cr10, Cr25, Cr50, and Cr75, respectively, when 70%, 85%, 91%, 97%, and 99% of **Va** disappeared, respectively. These yields became smaller with increasing initial concentration of **Cr**, which suggests that the increase suppressed the reaction between **Va** and $\mathbf{QM_{Va}}$ and hence

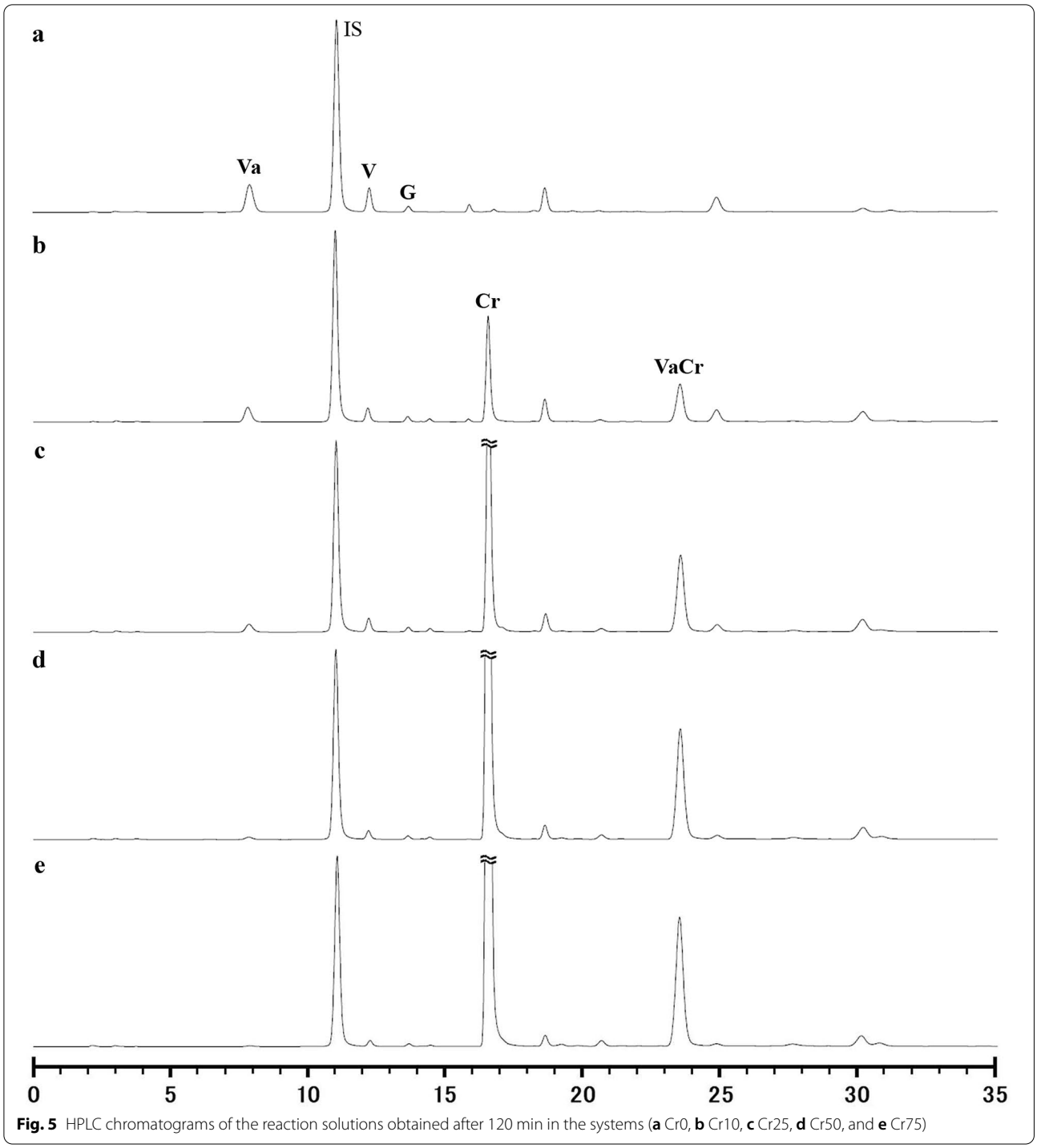

Fig. 5 HPLC chromatograms of the reaction solutions obtained after 120 min in the systems (**a** Cr0, **b** Cr10, **c** Cr25, **d** Cr50, and **e** Cr75)

supports the above-described formation route of **V**. The formation of **Cr** would accompany this disproportionation, although neither **Cr** nor **VaCr** was detected in system Cr0 (Fig. 5a). **G** is presumed to have formed when the α-1-type self-condensation followed a route whereby the σ-complex intermediate was generated and then the π-electron system of the aromatic nucleus originating from $\mathbf{QM_{Va}}$ abstracted the proton from the hydroxymethyl group originating from **Va** (Fig. 3). The reformation of $\mathbf{QM_{Va}}$ would accompany this route. The yields of **G** were 5.5% ($\pm$0.2), 4.4% ($\pm$0.1), 3.9% ($\pm$0.0), 2.7% ($\pm$0.1), and 2.4% ($\pm$0.2), based on the initial mole amount of **Va**

in the same reactions as described above for **V**. Those yields were also smaller with increasing initial concentration of **Cr**, which suggests that the increase suppressed the reaction between **Va** and $\mathbf{QM_{Va}}$ and hence supports the above-described formation route of **G**.

Detailed analysis of the disappearance of Va and formation of VaCr

Figure 6a, b, c, d, e shows the time courses of the changes in the concentrations of **Va**, **Cr**, and **VaCr** in systems Cr0, Cr10, Cr25, Cr50, and Cr75, respectively. Figure 6f, g, h shows those in the recovery yields of **Va**, **Cr**, and in the yields of **VaCr**, respectively, in these systems based on the initial amounts of **Va**, **Cr**, and **Va**, respectively.

Cr hardly disappeared when it was treated as the sole compound under the same conditions as the systems employed in this work, which shows its high stability under the employed conditions and also the complete absence of oxygen from the system judging from the lability of **Cr** to oxygen oxidation under alkaline conditions [25]. In spite of this, the mole amounts of disappearing **Cr** were roughly about 1.5 times larger than those of the generated **VaCr**, the only exclusive condensation product identified in this work, at a reaction time of 120 min in most runs. This phenomenon cannot currently be explained. **Cr** may have condensed with some compounds to afford products other than **VaCr**, although such condensations do not seem to have afforded any major products. These minor products will be identified in our forthcoming paper.

The yields of **VaCr** monotonically increased in all the systems and seem to have approached ceiling levels, indicating that **VaCr** does not frequently condense further as a nucleophile and is rather stable. The ceiling levels seemed to be 20–25%, 40–45%, 55–60%, and 65–70% in systems Cr10, Cr25, Cr50, and Cr75, respectively, although **Va** still remained with yields of 14.7% (±0.8) and 5.7% (±0.0) in the former two systems, respectively, at a reaction time of 120 min. These levels and the ratios of the initial amounts between **Va** and **Cr** suggest that the self-condensation of **Va** (as well as the disproportionation) progresses more readily than the condensation between **Va** and **Cr**. It should be noted that there are several routes for self-condensation, and not a major but many minor products form. Although the self-condensation of **Va** consumes more **Va** than the condensation between **Va** and **Cr**, the yield of **VaCr** at a reaction time of 120 min in system Cr10 was much lower than the half amount of consumed **Va** based on the initial amount of **Va** (43%). The ceiling levels in the other systems also seem to indicate more labile progress of the self-condensation of **Va**.

There must be some factors that promote self-condensation, because the electron density of the aromatic nucleus, which is a factor commonly used to judge the reactivity of an aromatic nucleus as a nucleophile, is not largely different between **Va** and **Cr**, and hence the aromatic nuclei of **Va** and **Cr** should have similar reactivities as nucleophiles. Two possible factors are as follows: (i) **Va** can additionally condense at its aromatic C-1 position owing to the presence of the benzyl hydroxy group; and

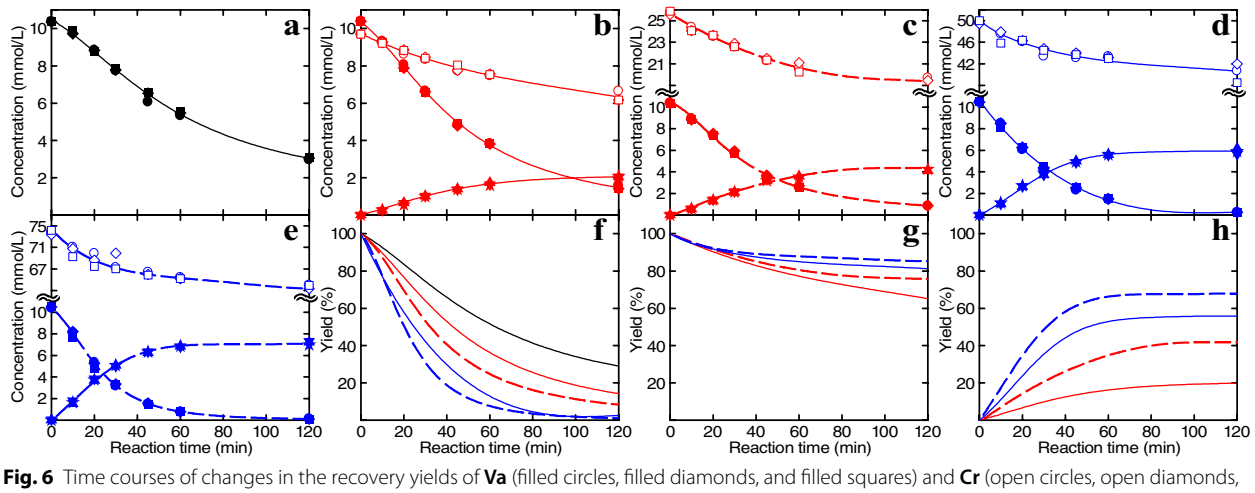

Fig. 6 Time courses of changes in the recovery yields of **Va** (filled circles, filled diamonds, and filled squares) and **Cr** (open circles, open diamonds, and open squares), and yield of **VaCr** (filled stars, filled triangles, and filled inverted triangles) in the systems [**a** Cr0 (solid black lines), **b** Cr10 (solid red lines), **c** Cr25 (dotted red lines), **d** Cr50 (solid blue lines), and **e** Cr75 (dotted blue lines)], and in the recovery yields of **Va** (**f**) and **Cr** (**g**), and in the yield of **VaCr** (**h**). Filled circles, open circles, and filled stars show the 1st trial. Filled diamonds, open diamonds, and filled triangles show the 2nd trial. Filled squares, open squares, and filled inverted triangles show the 3rd trial.

(ii) Dimers produced by the self-condensation of **Va** can further condense to be larger self-condensation products, resulting in acceleration of the disappearance of **Va**. It is one of our research topics to examine what factors actually promote the self-condensation of **Va**. Kinetic analyses are required to quantitatively compare the reactivities between **Va** and **Cr** as nucleophiles toward $\mathbf{QM_{Va}}$.

Although self-condensation products larger than dimers were produced, and the disproportionation would reproduce $\mathbf{QM_{Va}}$ in system Cr0, it was noteworthy that the disappearance rate of **Va** approximated to a common second-order reaction rate equation: $-d[\mathbf{Va}]_t/dt = k_{Cr0}[\mathbf{Va}]_t^2$ ($[\mathbf{Va}]_t$: concentration of **Va** at a reaction time of t, k_{Cr0}: second-order reaction rate constant). Because the reaction period before 20 min involves a temperature increase [26–28] and the remaining yield of **Va** at a reaction time of 120 min could be too low for inclusion in the approximation, the data points at reaction times of 20, 30, 45 and 60 min were employed. The k_{Cr0} value obtained by three duplicate runs was 1.77 ± 0.10 L mol^{-1} min^{-1}, with three squared correlation coefficients (R^2) in each run: 0.992, 0.997, and 0.997. The major reaction in system Cr0 can thus be the self-condensation between two molecules of **Va**.

Not only all reactions occurring in system Cr0 but also the condensation between **Va** and **Cr** to afford **VaCr** could progress in systems Cr10, Cr25, Cr50, and Cr75, in addition to other minor reactions. Therefore, the disappearance rates of **Va** could have been expressed well by a second-order reaction rate equation: $-d[\mathbf{Va}]_t/dt = k_{Cr0}[\mathbf{Va}]_t^2 + k[\mathbf{Va}]_t[\mathbf{Cr}]_t$ ($[\mathbf{Cr}]_t$: concentration of **Cr** at a reaction time of t, k: second-order reaction rate constant). However, the approximations employing the data points at reaction times of 20, 30, 45 and 60 min were poor in all the systems. When the k value was individually calculated at each of these four reaction times, it increased with the progress of the reaction (0.601–1.27, 0.460–0.925, 0.479–0.850, or 0.203–0.823 L mol^{-1} min^{-1} in system Cr10, Cr25, Cr50, or Cr75, respectively) and showed the maximum value at a reaction time of 45 min. Although the term, $k[\mathbf{Va}]_t[\mathbf{Cr}]_t$, in the above equation is expressed only by the concentrations of **Va** and **Cr**, it actually connotes the rate of the disappearance of **Va** caused by not only the condensation between **Va** and **Cr** but also all reactions that did not occur in system Cr0 but progressed in the other systems owing to the co-presence of **Cr**. It is thus suggested that the latter kind of reaction becomes more favorable with the progress of the reactions in these systems. The k values became smaller with increasing initial concentration of **Cr**, which suggests that the latter kind of reaction becomes favorable with a degree smaller than that expected from the increase in the initial concentration. As even the maximum values were smaller than the k_{Cr0}, the rate constant of the former term in the right side of the equation, it can be safely concluded that the self-condensation of **Va** progresses more readily than the condensation between **Va** and **Cr** even in the systems containing **Cr**.

Because **VaCr** did not clearly decrease after its formation, as shown in Fig. 6h, the formation rates of **VaCr** could have been expressed well by a second-order reaction rate equation: $d[\mathbf{VaCr}]_t/dt = k'[\mathbf{Va}]_t[\mathbf{Cr}]_t$ (k': second-order reaction rate constant). The approximations employing the data points at reaction times of 20, 30, 45 and 60 min were not good either, although the deviations were smaller than those in the previous approximations. When the k' value was individually calculated at each of these four reaction times, the k' values at these times were in ranges of: 0.515–0.678, 0.512–0.567 (0.147 at 60 min), 0.452–0.544, or 0.418–0.588 (0.231 at 60 min) in system Cr10, Cr25, Cr50, or Cr75, respectively. The k' values seem to be smaller with increasing initial concentration of **Cr**. Because the formation rate of **VaCr** would be the proportional connection to initial concentration of **Cr** when the k' values are constant regardless of the initial concentration, the formation of **VaCr** is accelerated by increasing the initial concentration to a degree smaller than the proportional connection. The ceiling levels of the formation of **VaCr** estimated from Fig. 6h also seem to show this phenomenon. Because the k' values of the ranges were about 1/4–1/3 of the k_{Cr0} value, the formation of **VaCr** was slower than the self-condensation of **Va**. This is partly because self-condensation consists of not the only route affording the α-5-type product but also routes generating the α-1-type, other dimers, and products larger than dimers, as described above. The k' value contrarily corresponds to the only reaction route affording the α-5-type condensation product between **Va** and **Cr**, **VaCr**. Identification and quantification of the self-condensation products of **Va** are required to compare the formation rates between possible condensation reactions.

Effect of temperature on the condensation between Va and Cr

Figure 7a, b, c shows the time courses of the changes in the concentrations of **Va**, **Cr**, and **VaCr** in systems 130, 150, and 170, respectively. System 150 is identical to system Cr50. Figure 7d, e, f shows those in the recovery yields of **Va**, in those of **Cr**, and in the yields of **VaCr** in these systems, respectively, based on the initial mole amounts of **Va**, **Cr**, and **Va**, respectively.

The disappearances of **Va** and **Cr** and formation of **VaCr** were naturally more rapid with rising temperature. The ceiling levels of formation of **VaCr** at 150 °C and 170 °C were about 60%, based on the initial mole amount of **Va**. Because the ratio of the formation amount of **VaCr**

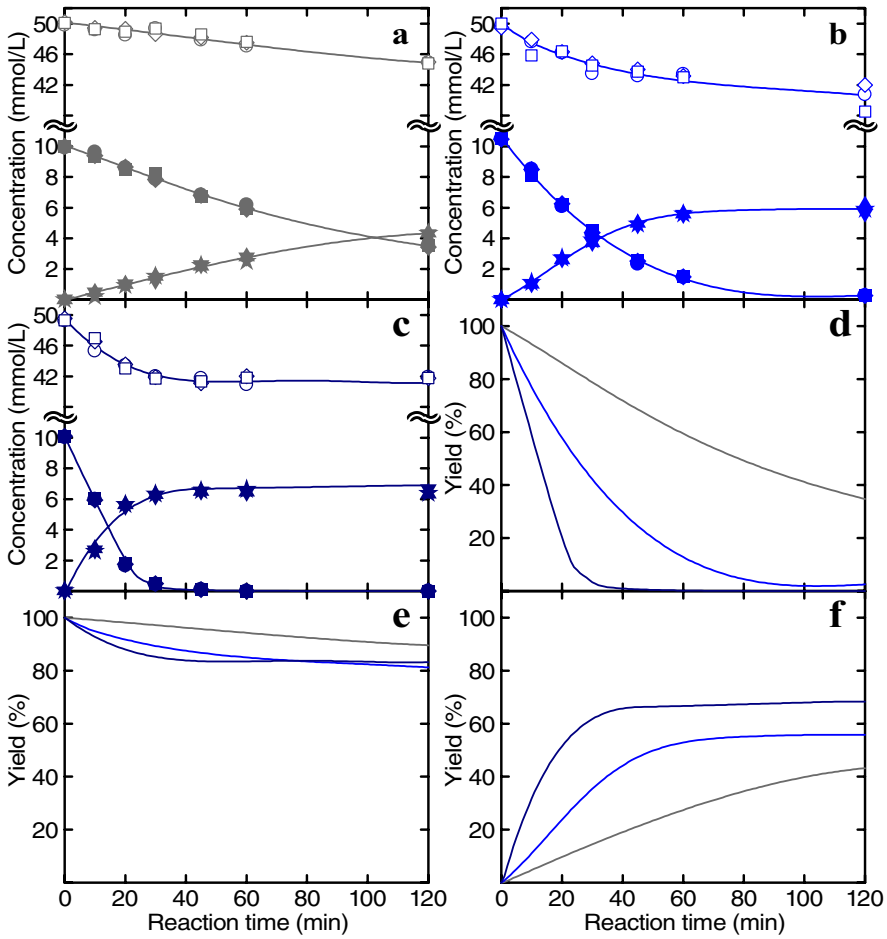

Fig. 7 Time courses of the changes in the recovery yields of **Va** (filled circles, filled diamonds, and filled squares) and **Cr** (open circles, open diamonds, and open squares), and yield of **VaCr** (filled stars, filled triangles, and filled inverted triangles) in the systems. **a** 130 (solid grey lines), **b** 150 (solid blue lines), and **c** 170 (solid dark blue lines), and in the recovery yields of **Va** (**d**) and **Cr** (**e**), and in the yield of **VaCr** (**f**). Filled circles, open circles, and filled stars show the 1st trial. Filled diamonds, open diamonds, and filled triangles show the 2nd trial. Filled squares, open squares, and filled inverted triangles show the 3rd trial.

to the disappearing amount of **Va** seems to be also about 60% during the whole reaction at 130 °C, the ceiling level can also be about 60% at 130 °C. The consumption of **Cr** was thus greater than the formation amount of **VaCr** at any temperature.

When a pseudo-first-order reaction can be applied to the approximation of the disappearance of **Va**, the change in the concentration of **Cr** during the reaction should be negligible or much smaller than that of **Va**. Although the concentrations of **Cr** clearly decreased at all temperatures, as shown in Fig. 7e, a pseudo-first-order reaction rate equation: $-d[\mathbf{Va}]_t/dt = k_{\mathrm{obs}}[\mathbf{Va}]_t$ (k_{obs}: pseudo-first-order reaction rate constant) was applied to the approximation of the disappearance rates of **Va** on trial. Table 2 lists the values of k_{obs} and R^2 in three duplicate runs. As a result, all the approximations were good. The Arrhenius activation energy (E_{a}) and frequency factor (A) were

Table 2 Pseudo-first-order reaction rate constants (k_{obs}) observed in systems 130, 150, and 170 and squared correlation coefficients (R^2) in all the runs in the approximations to the pseudo-first-order reaction rate equation

System	k_{obs} ($\times 10^{-2}$ min^{-1})[a]	R^2
130	0.881 ± 0.056	0.994
		0.994
		0.975
150	3.60 ± 0.13	0.997
		1.00
		0.999
170	11.4 ± 0.3	0.993
		0.997
		0.998

[a] The values after the '±' marks are standard deviations obtained from three duplicate runs

obtained by preparing an Arrhenius plot. The values were 95.3 kJ/mol and 2.02×10^{10} min^{-1}, respectively. When these values were calculated for the *β-O*-4 bond cleavage of the *erythro* and *threo* isomers of a non-phenolic lignin model compound under soda cooking conditions employing a NaOH concentration of 1.0 mol/L in our previous report [26], the values were 130 kJ/mol and 2.94×10^{14} min^{-1}, respectively, for the *erythro* isomer, and 133 kJ/mol and 1.66×10^{14} min^{-1}, respectively, for the *threo* isomer. The k_{obs} values obtained in this work do not correspond to a specific condensation reaction but comprehensively to the whole set of reactions occurring in the systems, while those in our previous report were specifically for the *β-O*-4 bond cleavage reaction. Nevertheless, a comparison of the E_a and A values between this and our previous reports should have some meaning. The E_a value obtained in this work is smaller than that in our previous report, which indicates that the k_{obs} value varied with temperature less significantly in this work than in our previous report. The A value obtained in this work is smaller than that in our previous report, which indicates that the k_{obs} value in this work is smaller than that in our previous report in a high-temperature region. These findings suggest that condensation can progress more rapidly than *β-O*-4 bond cleavage in a relatively low-temperature region, although no concrete temperature region can yet be described. Temperature may have to be raised to the maximum as quickly as possible in a soda cooking process to minimize condensation.

Conclusions

The condensation reaction of lignin was quantitatively examined in the simplest model systems: phenolic lignin model compounds, **Va** and **Cr**, were treated together under soda cooking conditions with various different initial concentrations of **Cr**. The *α*-5-type condensation product between these compounds, **VaCr**, was isolated and identified in accordance with previous reports. The quantitative analyses in this work showed that **VaCr** is the exclusive condensation product and rather stable under these conditions. The yields were 24%, 46%, 62%, or 72% based on the mole amount of disappearing **Va** at a reaction time of 120 min when the ratio of initial mole amount of **Cr** to that of **Va** was 1.0, 2.5, 5.0, or 7.5, respectively. These yields are not high enough to say that the condensation between these compounds is the exclusive major reaction in the systems. This fact and the comparison with the treatment of **Va** as the sole compound suggested that the self-condensation of **Va** progresses more readily than the condensation between **Va** and **Cr**, even in the system containing the largest amount of **Cr**, affording various minor condensation products.

The same treatments at three different temperatures, 130 °C, 150 °C, or 170 °C, may suggest that the condensation reaction progresses more rapidly than *β-O*-4 bond cleavage in a relatively low-temperature region in the soda cooking process, and hence the temperature should be raised to the maximum as soon as possible.

Abbreviations

Cr: Creosol; Cr: Creosol as a label; **G**: Guaiacol; IS: Internal standard compound; QM: Quinone methide structure; *o*-QM: *Ortho*-Type quinone methide structure; $\mathbf{QM_{Va}}$: The QM derived from **Va**; **V**: Vanillin; **Va**: Vanillyl alcohol; Va: Vanillyl alcohol as a label; **VaCr**: The *α*-5-type condensation product between **Va** and **Cr** (2-(4-hydroxy-3-methoxybenzyl)-6-methoxy-4-methylphenol).

Supplementary Information

The online version contains supplementary material available at https://doi.org/10.1186/s10086-021-01978-4.

Additional file 1: Figure S1. ^{13}C-NMR and DEPT135 spectra of **VaCr**. **Figure S2.** Aromatic region of ^{1}H-^{1}H COSY NMR spectrum of **VaCr**. **Figures S3–S6.** ^{1}H-^{13}C HSQC NMR spectrum of **VaCr**. **Figures S7–S11.** ^{1}H-^{13}C HMBC NMR spectrum of **VaCr**. **Table S1.** Assignments of the ^{1}H-NMR and MS spectra of isolated and identified **V**.

Acknowledgements

The authors gratefully acknowledge suggestions and discussion from Dr. Yuji Matsumoto and Dr. Takuya Akiyama.

Authors' contributions

TK conducted the experiments, analyzed the obtained data, and wrote the draft of this manuscript under the supervision of TY. TY completed the final manuscript. Both authors read and approved the final manuscript.

Availability of data and materials

The datasets used and/or analyzed during the current study are available from the corresponding author on reasonable request.

Declarations

Ethics approval and consent to participate

Not applicable.

Consent for publication

Not applicable.

Competing interests

The authors declare that they have no competing interests.

Received: 16 March 2021 Accepted: 1 June 2021
Published online: 09 June 2021

References

1. Gierer J, Imsgard F, Pettersson I (1976) Possible condensation and polymerization reactions of lignin fragments during alkaline pulping processes. Appl Polym Symp 28:1195–1211
2. Gierer J, Pettersson I (1977) Studies on the condensation of lignins in alkaline media part II: the formation of stilbene and arylcoumaran structures through neighboring group participation reactions. Can J Chem 55:593–599

3. Gierer J, Ljunggren S (1979) The reactions of lignin during sulfate pulping part 17: kinetic treatment of the formation and competing reactions of quinone methide intermediates. Svensk Papperstidn 82:503–512
4. Gierer J (1985) Chemistry of delignification part 1: general concept and reactions during pulping. Wood Sci Technol 19:289–312
5. Kratzl K, Wagner I (1972) Modellversuche zur kondensation des lignins 2: Mitt. zur vollständigen methylierung von ligninen und modellen; über Kondensationsreaktionen von phenolen mit formaldehyd und xylose. Holzforschung Holzverwertung 24:56–61
6. Francis DJ, Yeddanapalli LM (1962) Kinetics and mechanism of the alkali catalyzed condensation of *o*- and *p*-methylol phenols by themselves and with phenol. Makromol Chem 55:74–86
7. Yoon BH, Okada M, Yasuda S, Terashima N (1979) Chromophoric structures of alkali lignin I: reaction products from vanillyl alcohol with alkali. Mokuzai Gakkaishi 25:302–307
8. Dimmel DR, Shepard D, Brown TA (1981) The influence of anthrahydroquinone and other additives on the condensation reactions of vanillyl alcohol. J Wood Chem Technol 1:123–146
9. Smith DA, Dimmel DR (1994) Electron transfer reactions in pulping systems (IX): reactions of syringyl alcohol with pulping reagents. J Wood Chem Technol 14:297–313
10. Yasuda S, Fujii K, Yoon BH, Terashima N (1979) Chromophoric structures of alkali lignin II: chromophoric structures of condensation products from vanillyl alcohol. Mokuzai Gakkaishi 25:431–436
11. Fullerton T (1987) The condensation reactions of lignin model compounds in alkaline pulping liquors. J Wood Chem Technol 7:441–462
12. Gierer J, Söderberg S, Thorén S (1963) On the reactions of lignin during sulphate cooking part IV: stability of diphenylmethane structures under the conditions of alkali and sulphate cooking. Svensk Papperstidn 66:990–992
13. Xu H, Lai YZ (1999) Reactivity of lignin diphenylmethane model dimers under alkaline pulping conditions. J Wood Chem Technol 19:1–12
14. Gierer J, Ljunggren S (1983) Comparative studies of the participation of different neighboring groups in the alkaline cleavage of β-aryl ether bonds in lignins. Svensk Papperstidn 86:R100–R106
15. Funaoka M (1998) A new type of phenolic lignin-based network polymer with the structure-variable function composed of 1,1-diarylpropane units. Polym Int 47:277–290
16. Nagamatsu N, Funaoka M (2003) Design of recyclable matrixes from lignin-based polymers. Green Chem 5:595–601
17. Nonaka H, Yamamoto R, Funaoka M (2016) Selective conversion of hardwood lignin into syringyl methyl benzofuran using *p*-cresol. Polym J 48:977–981
18. Nonaka H, Yamamoto R, Katsuzaki H, Funaoka M (2016) Suggested production of a guaiacyl benzofuran derivative from softwood *via* lignocresol. BioResources 11:6932–6939
19. Hata T, Nonaka H (2018) Dilute acid hydrolysis of *p*-cresol-impregnated wood meal. Biomass Conv Bioref 8:339–343
20. Hata T, Nonaka H (2019) Fractionation of woody biomass with impregnation of monophenol by prehydrolysis and the subsequent soda cooking. Bioresour Technol Rep 5:178–184
21. Leary G, Yap CY (1977) Reactive lignin intermediates. VI. Oxidation and coupling of isoeugenol with a quinone methide. Aust J Chem 30:2323–2327
22. Leary G (1980) Quinone methides and the structure of lignin. Wood Sci Technol 14:21–34
23. Holmgren A, Brunow G, Henriksson G, Zhang L, Ralph J (2006) Non-enzymatic reduction of quinone methides during oxidative coupling of monolignols: implications for the origin of benzyl structures in lignins. Org Biomol Chem 4:3456–3461
24. Kubo S, Hashida K, Hishiyama S, Yamada T, Hosoya S (2015) Possibilities of the formation of enol-ethers in lignin by soda pulping. J Wood Chem Technol 35:62–72
25. Yokoyama T, Matsumoto Y, Meshitsuka G (2007) Detailed examination of the degradation of phenol derivatives under oxygen delignification conditions. J Agric Food Chem 55:1301–1307
26. Shimizu S, Yokoyama T, Akiyama T, Matsumoto Y (2012) Reactivity of lignin with different composition of aromatic syringyl/guaiacyl structures and *erythro*/*threo* chain structures in β-*O*-4 type during alkaline delignification: as a basis for the different degradability of hardwood and softwood lignin. J Agric Food Chem 60:6471–6476
27. Shimizu S, Posoknistakul P, Yokoyama T, Matsumoto Y (2013) Quantitative difference in the rates of the β-*O*-4 bond cleavage between lignin model compounds with and without γ-hydroxymethyl groups during the alkaline pulping process. BioResources 8:4312–4322
28. Shimizu S, Yokoyama T, Matsumoto Y (2015) Effect of type of aromatic nucleus in lignin on the rate of the β-*O*-4 bond cleavage during alkaline pulping process. J Wood Sci 61:529–536

Publisher's Note